

# A posteriori Trading-inspired Model-free Time Series Segmentation

Mogens Graf Plessen

**Abstract**—Within the context of multivariate time series segmentation this paper proposes a method inspired by a posteriori optimal trading. After a normalization step time series are treated channel-wise as surrogate stock prices that can be traded optimally a posteriori in a virtual portfolio holding either stock or cash. Linear transaction costs are interpreted as hyperparameters for noise filtering. Resulting trading signals as well as resulting trading signals obtained on the reversed time series are used for unsupervised labeling, before a consensus over channels is reached that determines segmentation time instants. The method is model-free such that no model prescriptions for segments are made. Benefits of proposed approach include simplicity, computational efficiency and adaptability to a wide range of different shapes of time series. Performance is demonstrated on synthetic and real-world data, including a large-scale dataset comprising a multivariate time series of dimension 1000 and length 2709. Proposed method is compared to a popular model-based bottom-up approach fitting piecewise affine models and to a recent model-based top-down approach fitting Gaussian models, and found to be consistently faster while producing more intuitive results.

## I. INTRODUCTION

Analysis of multivariate time series data is relevant in every engineering field. An ongoing increase in sensors employment simultaneously implies a rise in measurement data generation. Once a multivariate data point is measured it can either be processed isolatedly or in combination with a sequence of previous measurements. Given such a sequence a natural task is to segment it. Thus, the problem addressed in this paper is to partition multivariate time series data into segments such that different segments exhibit different and characteristic behavior.

The importance of time series segmentation stems from the fact that it is essential to manage large amounts of multivariate data, and that it can form the foundation for further upstream time series analysis tasks such as clustering, compression or forecasting. Note that the problem of time series segmentation is closely related to, and often interchangeably implied by a variety of problems labeled in the literature as “changepoint detection”, “breakpoint detection” or “event detection”. For example, segment boundaries can be interpreted as changepoints or breakpoints where characteristic behavior changes.

Algorithms for time series segmentation can be classified according to four criteria. First, the *number of segments* is either prescribed by a hyperparameter choice, or, alternatively, optimized in addition to the time instants defining the segmentation. Second, each segment may be fitted by a specific *segment model* (e.g., a piecewise affine or Gaussian model), or, alternatively, no specific model fit may be prescribed. For the former case, it can be further differentiated between

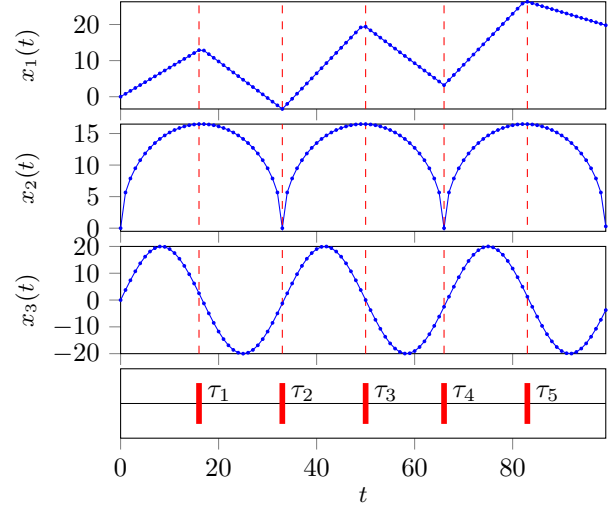


Fig. 1. Problem sketch. Given a multivariate time series (blue) suitable segmentation time instants (red dashed) are sought. In this paper, a method inspired by a posteriori optimal trading is proposed that identifies local maxima and minima channel-wise for each  $\{x_i(t)\}_{t=0}^T, \forall i = 1, \dots, n_x$  and for their reversed time series, before a unifying consensus over all channels is reached resulting in time instants  $\{\tau_k\}_{k=1}^K$ . For example, for  $n_x = 3$  and a uniformly-weighted consensus over all three channels the result is obtained as illustrated, even though the third channel’s local maxima and minima are phase-shifted with respect to the other two channels.

### MAIN NOMENCLATURE

<b>Symbols</b>	
$b_i(t)$	Binary state for channel $i$ at time $t$ .
$b_i^*(t)$	Optimal binary state for channel $i$ at time $t$ .
$\epsilon_i$	Transaction cost level for channel $i$ .
$\epsilon^{\min}, \epsilon^{\max}$	Minimum and maximum constraint on $\epsilon_i$ .
$\gamma^\bullet$	Hyperparameters for APTS, $\bullet \in \{\text{mult, close, plat}\}$ .
$n_x$	Dimension of multivariate time series.
$q^*(t)$	Optimal binary consensus state at time $t$ .
$\{\tau_k\}_{k=1}^K$	Identified list of segmentation time instants.
$\{\tau_k^{\text{flip}}\}_{k=1}^K$	Segmentation obtained on reversed time series.
$u_i(t)$	Binary control for channel $i$ at time $t$ .
$x(t)$	Multivariate time series data point at time $t$ .
$\tilde{x}_i(t)$	Data point for channel $i$ at time $t$ .
$\tilde{x}_i(t)$	Data point after normalization.
$z_i(t)$	Four-dimensional state vector.
$\hat{K}$	Identified number of segments.
$K^{\max}$	Maximum permissible number of segments.
$T$	Length of multivariate time series.
<b>Functions</b>	
$\mathcal{F}^{\text{normalize}}(\cdot)$	Mapping from $\{x_i(t)\}_{t=0}^T$ to $\{\tilde{x}_i(t)\}_{t=0}^T$ .
$\mathcal{F}^{\text{trade}}(\cdot)$	Mapping from $\{\tilde{x}_i(t)\}_{t=0}^T$ to $\{b_i^*(t)\}_{t=0}^T$ .
$\mathcal{F}^{\text{consensus}}(\cdot)$	Mapping from $\{b_i^*(t)\}_{t=0}^T, i=1, \dots, n_x$ to $\{q^*(t)\}_{t=0}^T$ .
$\mathcal{F}^{\text{terminate}}(\cdot)$	Mapping from $\{b_i^*(t)\}_{t=0}^T$ and $K^{\max}$ to a binary.
$\mathcal{F}^{\text{merge}}(\cdot)$	Mapping for merging of $\{\tau_k\}_{k=1}^{\hat{K}}$ and $\{\tau_k^{\text{flip}}\}_{k=1}^{\hat{K}}$ .
$\mathcal{F}^{\text{epsilon}}(\cdot)$	Mapping for determining transaction cost level $\epsilon_i$ .
<b>Abbreviations</b>	
BU	Bottom-Up Algorithm [1].
GGs	Greedy Gaussian Segmentation Algorithm [2].
APTS	A Posteriori Trading-inspired Segmentation.

the cases of (i) fitting the same model class to all segments but with different parameters, or (ii) fitting each segment by a model selected from a set of different model classes. Third, for the *algorithm type* it can be differentiated between batch offline or recursive online computation. Fourth, for the *machine learning type* it can be distinguished between supervised and unsupervised methods. For surveys on the topic see [3]–[5]. Supervised methods require a training phase to learn a classifier [6]–[8]. For example, a binary classifier distinguishes a “transition state” (change point) and a “within-state”. See also [9] for evolutionary time series segmentation using pattern templates. In contrast, unsupervised methods deal with unlabeled data. There exists a large variety of approaches, ranging from subspace [10], to probabilistic [11], segment-fitting [12], kernel-based [13], deep learning-based [14], graph-based [15] and density ratio methods [16], [17]. For a method assuming a fixed number of segments see, e.g., [18]. A variety of different segment model classes have been proposed, including also a model-free approach working with a dissimilarity matrix for single pattern change detection within the remote sensing domain [19], Fourier transforms [20], wavelets [21], piecewise affine representations [1], [22], and multivariate Gaussians [2].

Within this context the motivation and contribution of this paper is to present a simple and fast method that (i) does not assume a fixed number of change points, (ii) does not assume any specific segment model, (iii) is used for batch computation, (iv) is an unsupervised algorithm, (v) parallelizable, (vi) library-free in the sense that no specific internal optimisation routine (such as, e.g., a least-squares solution or factorization) is required, (vii) exhibits simple-to-select hyperparameters, and (viii) is scalable to large multivariate time series data. The fundamental approach is based on ideas from a posteriori optimal trading [23]. After a normalization step time series are treated channel-wise as surrogate stock prices that can be traded optimally a posteriori in a virtual portfolio holding either stock or cash. Linear transaction costs are therefore interpreted as hyperparameters for noise filtering. Resulting trading signals as well as resulting trading signals obtained on the reversed time series are then used for unsupervised labeling, before a consensus over channels is reached that determines segmentation instants. To the author’s knowledge this approach has not been presented in the literature.

The remaining paper is organized as follows. The multivariate time series segmentation problem is formulated mathematically in §II. The proposed solution is presented in §III. Numerical results are evaluated in §IV and compared to a bottom-up method [1] and to a recent top-down Gaussians-fitting method [2] on synthetic as well as real-world datasets [24], before concluding with §V.

## II. PROBLEM FORMULATION

A multivariate time series of finite length is defined as  $x(t) \in \mathbb{R}^{n_x}$ ,  $\forall t = 0, \dots, T$ . Here,  $x(T) \in \mathbb{R}^{n_x}$  represents the data point measured last. Time-indices do not need to be uniformly spaced. Instead, data points are only assumed to be ordered. Indices do not necessarily need to represent time instants, but could also denote space indices (e.g., with

space along a road as the dependent variable), unitless indices or other indexing. In general, units can vary channel-wise, whereby notation  $x_i(t)$ ,  $\forall i = 1, \dots, n_x$  is employed.

The problem addressed is to partition the multivariate time series,  $\{x_i(t)\}_{t=0}^T$ ,  $\forall i = 1, \dots, n_x$ , into  $\hat{K} + 1$  segments defined by change points or ordered time instants,  $\{\tau_k\}_{k=1}^{\hat{K}}$ , with  $0 < \tau_1 < \dots < \tau_{\hat{K}} < T$  such that different segments exhibit different and characteristic behavior. Rather than constraining a fixed number of segments,  $\hat{K}$  shall here also be identified in addition to the segmenting time instants. A batch offline algorithm is developed. In this paper, no specific model shall be prescribed for any time series segment to not artificially limit the solution space. This is in contrast to model-based approaches such as, e.g., [1] and [2], where piecewise affine and Gaussian models are fitted as part of their segmentation logics, respectively.

## III. PROBLEM SOLUTION

### A. A Posteriori Trading-inspired Segmentation Algorithm

This paper builds on [23] where a posteriori optimal trading over multiple assets subject to constraints for diversification was discussed. Within the context of multivariate time series segmentation the proposed method can be interpreted as virtual or surrogate channel-wise optimal trading on normalized time series data and the reversed time series data subject to linear transaction costs that represent hyperparameters for noise filtering, before determining a consensus based on the trading signals for all channels to obtain  $\hat{K}$  and  $\{\tau_k\}_{k=1}^{\hat{K}}$ . Details are outlined in the following.

First, a normalization is carried out in order to obtain channel-wise positive time series data. As will be discussed at the end of this section, positivity is a prerequisite for proposed segmentation logic. The following linear transformation is employed,  $\tilde{x}_i(t) = x_i(t) + \tilde{x}_i^{\text{offset}}$ ,  $\forall t = 0, \dots, T$ ,  $\forall i = 1, \dots, n_x$ , with  $\tilde{x}_i^{\text{offset}} = |\min_{t \in \{0, \dots, T\}} x_i(t)| + 1$ . The bias ensures positivity. In the following, the mapping from  $\{x_i(t)\}_{t=0}^T$  to  $\{\tilde{x}_i(t)\}_{t=0}^T$  shall be abbreviated by  $\mathcal{F}^{\text{normalize}}(\{x_i(t)\}_{t=0}^T)$ .

Second, channel-wise surrogate wealth dynamics are introduced that model a virtual portfolio holding either a virtual cash position or the “stock” modeled by the channel-wise normalized time series. Therefore, a four-dimensional state vector is defined,  $z_i(t) = [n_i(t), c_i(t), b_i(t), w_i(t)]$ , where  $n_i(t) \geq 0$  models the number of shares held at time  $t$ ,  $c_i(t) \geq 0$  the cash position,  $b_i(t) \in \{-1, 1\}$  the binary state indicating full investment in cash or stock, respectively, and finally  $w_i(t) \geq 0$  denoting total wealth at time  $t$ . In contrast to regular stock trading for our surrogate setup the number of shares,  $n_i(t) \geq 0$ , is real-valued. At  $t = 0$  the state vector is initialized with  $z_i(0) = [0, \frac{\tilde{x}_i(0)}{1-\epsilon_i}, -1, \frac{\tilde{x}_i(0)}{1-\epsilon_i}]$ , where  $\epsilon_i \in [0, 1)$  is interpreted as a linear transaction cost level. This initialization implies an initial cash position sufficient to buy one share when accounting for transaction cost and is defined this way to avoid adding scaling hyperparameters. Then, introducing a control variable,  $u_i(t) \in \{-1, 1\}$ , state

transition dynamics are defined as,

$$z_i(t+1) = \begin{cases} \begin{bmatrix} 0 \\ c_i(t) \\ -1 \\ c_i(t) \end{bmatrix}, & \text{if } u_i(t) = -1, \\ \begin{bmatrix} \frac{c_i(t)(1-\epsilon_i)}{\tilde{x}_i(t)} \\ 0 \\ 1 \\ n_i(t+1)\tilde{x}_i(t+1) \end{bmatrix}, & \text{if } u_i(t) = 1, \end{cases} \quad (1)$$

for  $z_i(t) \in \{z_i(t) \in \mathbb{R}^4 : b_i(t) = -1\}$ , and

$$z_i(t+1) = \begin{cases} \begin{bmatrix} 0 \\ n_i(t)\tilde{x}_i(t)(1-\epsilon_i) \\ -1 \\ c_i(t+1) \end{bmatrix}, & \text{if } u_i(t) = -1, \\ \begin{bmatrix} n_i(t) \\ 0 \\ 1 \\ n_i(t)\tilde{x}_i(t+1) \end{bmatrix}, & \text{if } u_i(t) = 1, \end{cases} \quad (2)$$

for  $z_i(t) \in \{z_i(t) \in \mathbb{R}^4 : b_i(t) = 1\}$ . Combinedly, (1)-(2) model all four possible transitions between full cash and full stock investment subject to linear transaction costs.

Third, in a causal setting  $\tilde{x}_i(t+1)$  is not known at time  $t$ . However, in the batch setting it is available, which is equivalent to perfect one step-ahead knowledge a posteriori. Therefore, and due to the fact of a positive  $\tilde{x}_i(t)$  by above discussion there always exists a wealth-maximizing trading trajectory from  $t = 0$  to  $T$  as a function of transaction cost level  $\epsilon_i \geq 0$  such that  $w_i(T)$  is channel-wise maximized. This trajectory can be computed efficiently as follows.

Starting from  $z_i(0)$  defined above, at  $t = 1$  two possible states can result which differ by binary  $b_i(1) \in \{-1, 1\}$ . Let these two states be denoted by  $z_i^{(-1)}(1)$  and  $z_i^{(1)}(1)$ , respectively. Then, by Bellman's principle of optimality [25] and with the purpose of deriving the wealth-maximizing trading trajectory the following recursion can be implemented for all  $t \geq 1$ . When  $\tilde{x}_i(t+1)$  becomes available,  $z_i^{(-1)}(t)$  and  $z_i^{(1)}(t)$  branch out to a total of four different states according to (1)-(2). These are pruned to two by selecting the  $w_i(t+1)$ -maximizing solutions for each  $b_i(t+1) = -1$  and  $b_i(t+1) = 1$  such that  $z_i^{(-1)}(t+1)$  and  $z_i^{(1)}(t+1)$  are obtained, respectively. Their corresponding optimal parent states are further recorded, which shall be denoted by  $z_i^{(-1),\text{parent}}(t)$  and  $z_i^{(1),\text{parent}}(t)$ . This recursion is repeated until  $t = T$ . Given  $z_i^{(-1)}(T)$  and  $z_i^{(1)}(T)$  let  $b_i^*(T) = -1$  if  $w_i^{(-1)}(T) > w_i^{(1)}(T)$ , and  $b_i^*(T) = 1$  otherwise. Now, using the list of optimal parent states,  $\{z_i^{(-1),\text{parent}}(t)\}_{t=1}^{T-1}$  and  $\{z_i^{(1),\text{parent}}(t)\}_{t=1}^{T-1}$ , the optimal wealth-maximizing trading trajectory can be obtained by backpropagation, resulting in  $\{b_i^*(t)\}_{t=0}^T$ . In the following,  $\mathcal{F}^{\text{trade}}(\{\tilde{x}_i(t)\}_{t=0}^T, \epsilon_i)$  shall abbreviate the mapping from  $\{\tilde{x}_i(t)\}_{t=0}^T$  to  $\{b_i^*(t)\}_{t=0}^T$  as a function of transaction cost level  $\epsilon_i > 0$ .

So far, it was discussed how to transform time series data  $\{x_i(t)\}_{t=0}^T$  to  $\{\tilde{x}_i(t)\}_{t=0}^T$ , before computing binary  $\{b_i^*(t)\}_{t=0}^T$  as a function of scalars  $\epsilon_i \geq 0$ . Note that all of these steps can be parallelized channel-wise for all  $i = 1, \dots, n_x$ . It remains to discuss (i) how to reach consensus over all  $n_x$  channels in order to produce final segmentation instants,  $\{\tau_k\}_{k=1}^{\hat{K}}$ , and (ii) how to appropriately select hyperparameters  $\epsilon_i$ .

Here, it is proposed to reach consensus from a weighted average defined as follows,

$$q^*(t) = \sum_{i=1}^{n_x} \eta_i p_i b_i^*(t), \quad \forall t = 0, \dots, T, \quad (3)$$

with weights  $\eta_i \in [0, 1]$  such that  $\sum_{i=1}^{n_x} \eta_i = 1$ ,  $p_1 = 1$  and

$$p_i = \arg \max_{p_i \in \{1, -1\}} \sum_{t=0}^T |b_1^*(t) + p_i b_i^*(t)|, \quad \forall i = 2, \dots, n_x. \quad (4)$$

Several comments are made. First, as a special case and treated as the default below, uniform weighting implies  $\eta_i = \frac{1}{n_x}$ . Alternatively, non-uniform weights may be used for trading-off importance of different sensor channels. (For a financial analogy, consider stock indices that weight different components according to their market capitalizations.)

Second, the introduction of binary  $p_i \in \{-1, 1\}$  is motivated by a symmetry argument. Suppose two channels with time series that are *mirrored* with respect to the time-axis, i.e.,  $x_2(t) = -x_1(t)$ . Then,  $b_2(t) = -b_1(t)$  follows. Consequently, for  $q^*(t) = \sum_{i=1}^{n_x} \eta_i b_i^*(t)$  with  $\eta_i = \frac{1}{n_x}$  the result  $q^*(t) = 0$  is obtained. However, this clearly is undesired. This can be seen by considering, for example, a sawtooth function for  $x_1(t)$ , and  $x_2(t) = -x_1(t)$ . Then, no changepoints at all would be identified eventhough these clearly exist. Therefore, the solution in (3) is proposed, which resolves the symmetry issue. The reference prescription  $p_i = 1$  for  $i = 1$  is arbitrary. Any other  $i \in \{2, \dots, n_x\}$  would also serve. Note that the introduction of  $p_i$  only affects consensus finding over all channels. The optimal trading trajectories for individual channels are still determined independently from each other. As a detail, by defining binary  $b_i(t) \in \{-1, 1\}$ , rather than the more conventional  $b_i(t) \in \{0, 1\}$ , (4) can be evaluated by simple multiplication. By construction  $q^*(t) \in [-1, 1]$ . Then,  $\{\tau_k\}_{k=1}^{\hat{K}}$  is computed as the ordered list of time instants at which  $q^*(t)$  crosses the threshold-level 0 either from below or above. For multivariate time series segmentation this differentiation is sufficient. Since  $z_i(0)$  is initialized in a surrogate cash position and for a larger number of positive than negative  $p_i$ , the time instants listed in  $\{\tau_k\}_{k=1}^{\hat{K}}$  alternatingly indicate the start of an up-trending (weightedly averaged over all channels) and a down-trending multivariate time series segment, respectively. In the following,  $\mathcal{F}^{\text{consensus}}(\{\{b_i^*(t)\}_{t=0}^T\}_{i=1}^{n_x})$  shall abbreviate the consensus mapping from  $\{\{b_i^*(t)\}_{t=0}^T\}_{i=1}^{n_x}$  to  $\{\tau_k\}_{k=1}^{\hat{K}}$ .

For any given time series data the selection of a suitable transaction cost level,  $\epsilon_i$ , is a priori not obvious. Therefore, an iterative approach is proposed. In the first iteration it is set  $\epsilon_i = 0$ , which is typically appropriate for data with high

signal-to-noise ratio. In the second iteration it is set  $\epsilon_i = \epsilon^{\min}$ , where  $\epsilon^{\min} > 0$  is a hyperparameter. For all remaining iterations it is set  $\epsilon_i^{\text{new}} = \gamma^{\text{mult}} \epsilon_i$ , where multiplier  $\gamma^{\text{mult}} > 1$  is a hyperparameter and  $\epsilon_i^{\text{new}}$  denotes the transaction cost level for the next iteration. Denoting iteration numbers by  $j \geq 0$ , the mapping to determine  $\epsilon_i$  shall be abbreviated by  $\mathcal{F}^{\text{epsilon}}(\epsilon_i, \epsilon^{\min}, \epsilon^{\max}, \gamma^{\text{mult}}, j)$  in the following.

The result  $\{b_i^*(t)\}_{t=0}^T$  clearly is a function of  $\epsilon_i$ . Let the number of switches, i.e., the number of changes where  $b_i^*(t+1) \neq b_i^*(t)$ , be denoted by  $\mathcal{L}(\epsilon_i)$ . This is bounded by  $0 \leq \mathcal{L}(\epsilon_i) \leq T$ . Furthermore,  $\mathcal{L}(\epsilon_i)$  clearly is monotonously decreasing for increasing  $\epsilon_i$ . This follows from the state transitions according to (1)-(2) and the wealth-maximizing method to construct  $\{b_i^*(t)\}_{t=0}^T$ . This monotonicity can be exploited for defining a simple stopping criterion. If  $0 < \mathcal{L}(\epsilon_i) \leq K^{\max}$ , then the channel-wise  $\epsilon_i$ -iteration is stopped. Here,  $K^{\max} > 0$  defines a user-defined maximum permissible number of segments. In addition, the pathological case must be handled where  $\mathcal{L}(\epsilon_i)$  drops to zero during  $\epsilon_i$ -iterations. Then, the last  $\epsilon_i$ -solution yielding  $\mathcal{L}(\epsilon_i) > 0$  is returned. By construction this always implies  $\mathcal{L}(\epsilon_i) > K^{\max}$ . Therefore, for such cases an additional merging-routine is employed, which is, however, introduced further below after the discussion of also handling the *reversed* time series data. In the following, the binary mapping for terminating  $\epsilon_i$ -iterations shall be abbreviated by  $\mathcal{F}^{\text{terminate}}(\{b_i^*(t)\}_{t=0}^T, K^{\max})$ .

For the trading-inspired methodology the resulting trajectory,  $\{b_i^*(t)\}_{t=0}^T$ , clearly is a function of the ordering of time series data. Therefore, to generalize the *reversed* time series data is also treated, before results for both directions are merged. Regarding reversed time series data treatment, the same  $\epsilon_i$  is employed that was found iteratively for the original (non-reversed) time series. This selection is done for computational efficiency and justified since absolute-valued incremental changes are invariant with respect to data ordering. Resulting breakpoints shall be denoted by  $\{\tau_k^{\text{flip}}\}_{k=1}^{\hat{K}^{\text{flip}}}$ . Regarding final merging of  $\{\tau_k\}_{k=1}^{\hat{K}}$  and  $\{\tau_k^{\text{flip}}\}_{k=1}^{\hat{K}^{\text{flip}}}$ , three comments are made. First, in case two breakpoints are closer than a small hyperparameter,  $\gamma^{\text{close}} > 0$ , the two breakpoints are averaged. For perspective on the order of magnitude, in numerical experiments it was selected  $\gamma^{\text{close}} = \max(0.01T, 2)$ . Second, for an efficient implementation of the merging, one can exploit the fact that both lists  $\{\tau_k\}_{k=1}^{\hat{K}}$  and  $\{\tau_k^{\text{flip}}\}_{k=1}^{\hat{K}^{\text{flip}}}$  are already ordered and increasing. Furthermore, for both it typically holds that  $\hat{K} \ll T$  and  $\hat{K}^{\text{flip}} \ll T$ . For perspective, for the last experiment reported in this paper it is  $\hat{K} = 9$  and  $T = 2709$ . Third, after above method of merging, the number of breakpoints may still exceed a desired upper bound  $K^{\max} > 0$ . Then, closest breakpoints with respect to their predecessor are iteratively removed until the condition  $\hat{K} \leq K^{\max}$  is satisfied for the merged list. In the following, the full mapping implementing both merging and removal of close breakpoints shall be abbreviated by  $\mathcal{F}^{\text{merge}}(\{\tau_k\}_{k=1}^{\hat{K}}, \{\tau_k^{\text{flip}}\}_{k=1}^{\hat{K}^{\text{flip}}}, \gamma^{\text{close}}, K^{\max})$ .

Algorithm 1 summarizes above discussion for multivariate time series segmentation and is called APTS (A Posteriori Trading-inspired Segmentation).

---

### Algorithm 1: APTS

---

**Subfunctions :**  $\mathcal{F}^{\text{normalize}}(\cdot)$ ,  $\mathcal{F}^{\text{trade}}(\cdot)$ ,  $\mathcal{F}^{\text{consensus}}(\cdot)$ ,  
 $\mathcal{F}^{\text{epsilon}}(\cdot)$ ,  $\mathcal{F}^{\text{terminate}}(\cdot)$ ,  $\mathcal{F}^{\text{merge}}(\cdot)$ .

---

**Hyperparam.:**  $\epsilon^{\min}$ ,  $\epsilon^{\max}$ ,  $\gamma^{\text{mult}}$ ,  $\gamma^{\text{close}}$ ,  $K^{\max}$ .

---

**Data Input :**  $\{\{x_i(t)\}_{t=0}^T\}_{i=0}^{n_x}$ .

---

```

1 for  $i \in \{1, \dots, n_x\}$  do
2    $\{\tilde{x}_i(t)\}_{t=0}^T \leftarrow \mathcal{F}^{\text{normalize}}(\{x_i(t)\}_{t=0}^T)$ .
3    $\epsilon_i \leftarrow 0$ ,  $j \leftarrow 0$ .
4   while continue do
5      $\epsilon_i \leftarrow \mathcal{F}^{\text{epsilon}}(\epsilon_i, \epsilon^{\min}, \epsilon^{\max}, \gamma^{\text{mult}}, j)$ .
6      $\{b_i^*(t)\}_{t=0}^T \leftarrow \mathcal{F}^{\text{trade}}(\{\tilde{x}_i(t)\}_{t=0}^T, \epsilon_i)$ .
7     if  $\mathcal{F}^{\text{terminate}}(\{b_i^*(t)\}_{t=0}^T, K^{\max}) == \text{True}$  then
8       break.
9      $j \leftarrow j + 1$ .
10   $\{\tau_k\}_{k=1}^{\hat{K}} \leftarrow \mathcal{F}^{\text{consensus}}(\{b_i^*(t)\}_{t=0}^T)_{i=1}^{n_x}$ .


---


11   $\{\tilde{x}_i^{\text{flip}}(t)\}_{t=0}^T \leftarrow \mathcal{F}^{\text{normalize}}(\{x_i(t)\}_{t=T}^0)$ .
12  for  $i \in \{1, \dots, n_x\}$  do
13     $\{b_i^{*,\text{flip}}(t)\}_{t=T}^0 \leftarrow \mathcal{F}^{\text{trade}}(\{\tilde{x}_i^{\text{flip}}(t)\}_{t=0}^T, \epsilon_i)$ .
14   $\{\tau_k^{\text{flip}}\}_{k=1}^{\hat{K}^{\text{flip}}} \leftarrow \mathcal{F}^{\text{consensus}}(\{b_i^{*,\text{flip}}(t)\}_{t=0}^T)_{i=1}^{n_x}$ .


---


15   $\{\tau_k\}_{k=1}^{\hat{K}} \leftarrow \mathcal{F}^{\text{merge}}(\{\tau_k\}_{k=1}^{\hat{K}}, \{\tau_k^{\text{flip}}\}_{k=1}^{\hat{K}^{\text{flip}}}, \gamma^{\text{close}}, K^{\max})$ .


---


Final Result :  $\{\tau_k\}_{k=1}^{\hat{K}}$ .

```

---

Three additional comments are made. First, the dominating complexity of Algorithm 1 is linear in time series length and dimension, i.e.,  $\mathcal{O}(n_x T N_\epsilon)$ . The maximum number of  $\epsilon_i$ -iterations,  $N_\epsilon > 0$ , in Steps 3-9 can be determined analytically from the formula,  $\epsilon^{\min} \gamma^{\text{mult} N_\epsilon - 1} < \epsilon^{\max}$ .

Second, the necessity of a normalization method resulting in channel-wise positive time series data is motivated by counterexample. As part of (1), the wealth equation  $w_i(t+1) = n_i(t+1)\tilde{x}_i(t+1) = \frac{c_i(t)(1-\epsilon_i)}{\tilde{x}_i(t)}\tilde{x}_i(t+1)$  occurs. Suppose  $\tilde{x}_i(t) < 0$  and further  $\tilde{x}_i(t+1) < \tilde{x}_i(t)$ . Then, a drop in “stock” price from time  $t$  to  $t+1$  would imply an increase in wealth (due to the ratio of two negative numbers in  $w_i(t+1)$ ). This scenario would be undesired since misleading. It is avoidable by a normalization method rendering data positive. (This excludes the standard z-normalization technique [26].)

Finally, an extension of APTS is discussed. By design Algorithm 1 is particularly suitable to segment time series with different local maxima and minima. However, by adding a simple data pre- and post-processing step also time series exhibiting channel-wise quasi-constant values for prolonged periods of times (plateaus) can be handled efficiently. Therefore, a small hyperparameter  $\gamma^{\text{plat}} \geq 0$  is introduced (e.g.,  $\gamma^{\text{plat}} = 0.05$ ) that is used after normalization in Step 2 for downsampling. Thus, a reduced time series is produced,  $\{\tilde{x}_i(t)\}_{t=0}^{\hat{T}} \in \{\{x_i(t)\}_{t=0}^T : \tilde{x}_i(t) - \tilde{x}_i(t-1) > \gamma^{\text{plat}}, \forall t =$

$0, \dots, T$ }. The same filtering step is also applied analogously after Step 11 to the reversed time series. The effect is removal of plateau-like data parts. Then, after processing via  $\mathcal{F}^{\text{trade}}(\{\bar{x}_i(t)\}_{t=0}^T, \epsilon_i)$ , the previously removed time periods must be reinserted to recover the original time indexing and produce an adjusted  $\{b_i^*(t)\}_{t=0}^T$  in Step 6, and analogously in Step 13 for the reversed time series. This methodology permits to accurately identify start and end times of plateau-like segments in time series data.

### B. Two Comparative Algorithms from the Literature

Before reporting numerical results, two comparative algorithms from the literature are briefly discussed.

Based on the fundamental belief that underlying data in each segment can be well approximated by piecewise affine representations, according to [1] most time series segmentation algorithms can be grouped into one of three categories: *sliding window*-approaches (a segment is grown until exceeding some error bound and starting a new segment), *top-down*-approaches (a time series is recursively partitioned until a stopping criterion is met), and *bottom-up*-approaches (starting from the finest possible approximation, segments are merged until a stopping criterion is met). In the same reference it is found empirically that the bottom-up approach (BU) is most suitable. Therefore, BU according to [1] is here used for comparison. For BU and for the fitting of piecewise affine representations, local solutions of either linear interpolation or linear regression (least-squares) problems are required for each segment. In [1], the latter approach is used for final experiments. Here, for a Python implementation `numpy.linalg.lstsq`-solver is employed for the solution of least-squares problems. It is worthwhile noting that the original reference exclusively focused on one-dimensional time series data (i.e.,  $n_x = 1$ ) for empirical evaluation. In this paper, BU is altered for handling of multivariate time series by straightforward extension. As stopping criterion, a desired number of segments is prescribed. This number represents the only hyperparameter. Thus, as soon as sufficiently many segments are merged (starting from the finest possible approximation) BU stops.

In [2], a top-down algorithm labeled *Greedy Gaussian Segmentation* (GGs) is proposed. Fundamental belief is that underlying data in each segment can be explained as samples from a multivariate Gaussian distribution with constant mean and covariance for each segment. To determine breakpoints (i.e., segment boundaries) a covariance-regularized maximum likelihood objective function is formulated,

$$\max_{\tau_1, \dots, \tau_K} -\frac{1}{2} \sum_{k=1}^{K+1} (\tau_k - \tau_{k-1}) \log \det \left( S^{(k)} + \frac{\lambda I}{\tau_k - \tau_{k-1}} \right) - \dots - \lambda \text{Tr} \left( S^{(k)} + \frac{\lambda I}{\tau_k - \tau_{k-1}} \right)^{-1}, \quad (5)$$

with hyperparameter  $K$  indicating the number of breakpoints, regularization hyperparameter  $\lambda > 0$ , trace-operator  $\text{Tr}(\cdot)$ , empirical covariance  $S^{(k)} = \frac{1}{\tau_k - \tau_{k-1}} \sum_{t=\tau_{k-1}}^{\tau_k-1} (x(t) - \mu^{(i)})(x(t) - \mu^{(i)})^T$ , empirical mean  $\mu^{(i)} = \frac{1}{\tau_k - \tau_{k-1}} \sum_{t=\tau_{k-1}}^{\tau_k-1} x(t)$ , data  $x(t) \in \mathbb{R}^{n_x}$  and  $I$

denoting the identity matrix. By alternately adding new breakpoints and adjusting the position of all breakpoints (5) is maximized until no change of any breakpoint further improves the objective function that sums costs over all segments. GGS requires selection of two hyperparameters. These are the desired number of breakpoints,  $K > 0$ , and the regularization parameter,  $\lambda > 0$ , to enforce positive definite (invertible) estimated covariance matrices. Code for GGS is publicly available and taken from the authors' website to conduct below numerical experiments. Non-trivial library routines required for the implementation of GGS include `numpy.linalg.slogdet`, `numpy.linalg.inv` and `numpy.linalg.cholesky`-functions. For a fixed number of breakpoints,  $K > 0$ , the complexity is  $\mathcal{O}(KLn_x^3T)$  flops, where  $L$  is the average number of iterations required for adjusting breakpoints. While an upper bound on  $L$  is not known, it was observed empirically that it is modest when  $K$  is not too large [2]. The cubic complexity in the dimension of the multivariate time series  $n_x$  is underlined.

## IV. NUMERICAL RESULTS

### A. Selection of Experiments and Evaluation of Results

Experimental data was selected with the purpose of comparing BU [1], GGS [2], and APTS on (i) a variety of different shapes of time series data to analyze generalizability of these methods, and (ii) on a large-scale example to compare computational efficiencies. Therefore, in addition to two synthetic examples eight samples from the publicly accessible UCR time series archive [24] were selected. This combination enabled testing on time series data with piecewise-affine segments, half-circles, rising and falling segments with local maxima and minima, plateau-like segments, strongly fluctuating data with different noise levels, impulse-like data, noise-perturbed multivariate data, and large-scale data with  $n_x = 1000$  channels and length  $T = 2709$ .

Two methods for evaluation of results were considered: (i) manually determining "ground-truth" segmentation instants before evaluating an error metric, and (ii) a visual approach where all results are explicitly plotted for subjective inspection and evaluation by the reader. The first approach has several disadvantages. These include that determining a ground-truth is subjective to the selector's preference. Furthermore, summarizing performance by a single scalar error metric may insufficiently capture actual segmentation quality of algorithms. Therefore, the second visual approach is taken, which is also appropriate given the typical unsupervised nature of time series segmentation tasks. In addition, computational solve times are reported for each experiment.

### B. Selection of Hyperparameters

In order to demonstrate robustness of APTS and adaptability to different shapes of data a single set of hyperparameters is used throughout all experiments. This set is summarized in Table I. For emphasis of handling of data with plateau-like segments, results for Examples 4-6 are also reported for  $\gamma^{\text{plat}} = 0.05$ , besides the default solutions for  $\gamma^{\text{plat}} = 0$ .

APTS does not define a specific number of segments by a hyperparameter selection. Instead, an upper bound  $K^{\text{max}} > 0$

Symbol	Value
$\epsilon^{\min}$	0.01
$\epsilon^{\max}$	1
$\gamma^{\text{mult}}$	2
$\gamma^{\text{close}}$	$\max(0.01T, 2)$
$\gamma^{\text{plat}}$	0
$K^{\max}$	10

TABLE I. To demonstrate robustness of APTS and adaptability to various time series data a single set of hyperparameters is used throughout all Experiments 1-10. For special identification of plateau-like segments results for Experiments 4-6 are additionally reported for  $\gamma^{\text{plat}} = 0.05$ .

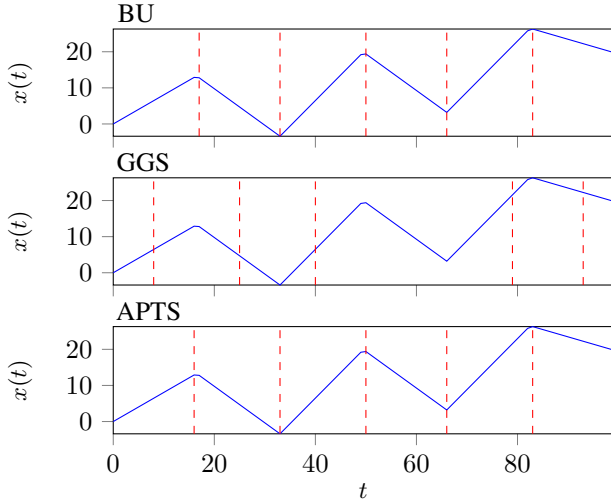


Fig. 2. Example 1. Results for synthetic one-dimensional time series data composed of piecewise affine segments. Vertical red dashed lines indicate identified segmentation indices.

must be provided, before Algorithm 1 returns  $\hat{K} \leq K^{\max}$ . In contrast, without adding on-top iterative selection methods BU and GGS require prescription of a desired number of segments  $K > 0$ . Therefore, in order to compare BU, GGS and APTS the following method is applied. First, APTS is run. Then, BU and GGS are run with setting  $K = \hat{K}$ . This permits a comparison for the same number of segments.

BU does not require a hyperparameter selection beyond  $K$ . In contrast, GGS additionally requires setting of the regularization hyperparameter  $\lambda > 0$  in (5). After empirical testing,  $\lambda = 10^{-1}$  was determined for Examples 1-9 and  $\lambda = 10^{-4}$  for Example 10. For the latter experiment  $\lambda$  had to be reduced in order to produce solutions with larger  $K$ . (The final result is obtained for  $K = 9$ .)

### C. Numerical Results

All methods were implemented in Python. All experiments were run on an Intel i7-7700K CPU@4.2GHz×8 processor with 15.6 GiB memory. Results for Examples 1-10 are visualized in Fig. 2-13. Computational solve times are summarized in Table II, and in Fig. 12 for Example 10.

Overall, APTS performs best and represents the most versatile approach for the handling of different shapes of time series data. While BU as expected appropriately segments the

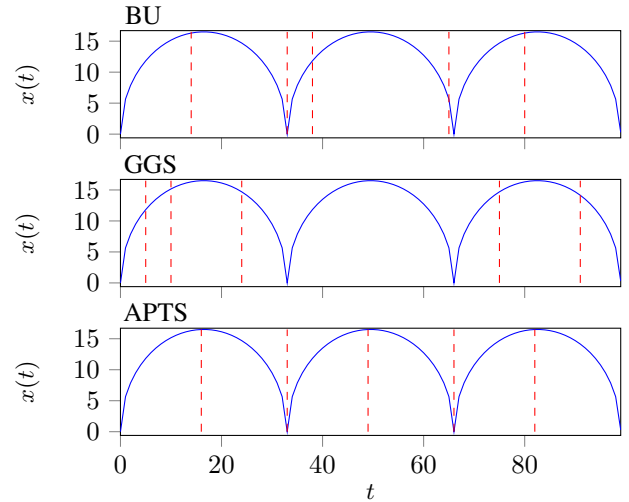


Fig. 3. Example 2. Results for synthetic one-dimensional time series data composed of half-circles.

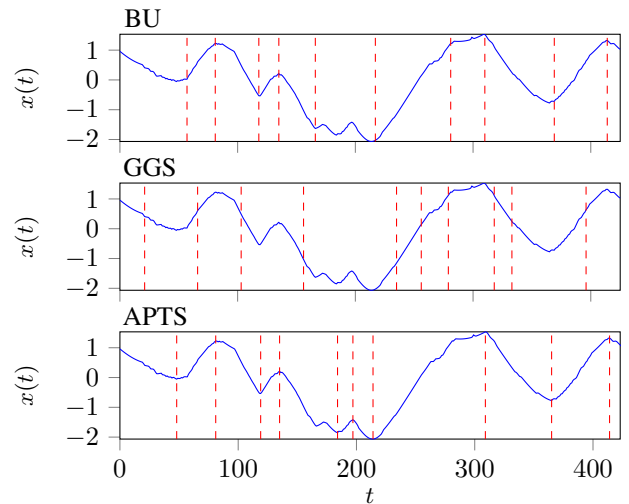


Fig. 4. Example 3. One-dimensional sample from dataset 'Yoga' [24].

piecewise affine time series in Fig. 2, BU fails for the time series of Fig. 3 with half-circle shapes. GGS is found to not be suitable for accurate identification of local maxima and minima. Instead, GGS seems to be best suited for data of varying amplitude or noise levels such as in the examples of Fig. 6-7. However, for  $\gamma^{\text{plat}} > 0$  these examples can be solved equally good by APTS and much faster. In fact, as Table II shows, APTS offers consistently smaller solve times throughout all experiments in comparison to BU and GGS. Furthermore, APTS is much better scalable to high-dimensional data as Fig. 12 demonstrates.

It is also found that the characteristic of APTS to return a solution for a prescribed upper bound  $\hat{K} \leq K^{\max}$ , rather than for a scalar prescribing an exact desired number of segments, is not to be seen as a disadvantage. On the contrary, this characteristic of APTS permits to solve all 10 examples with a single set of hyperparameters, to tailor a suitable  $\hat{K}$  for any given data, and thus to increase the degree of automation.

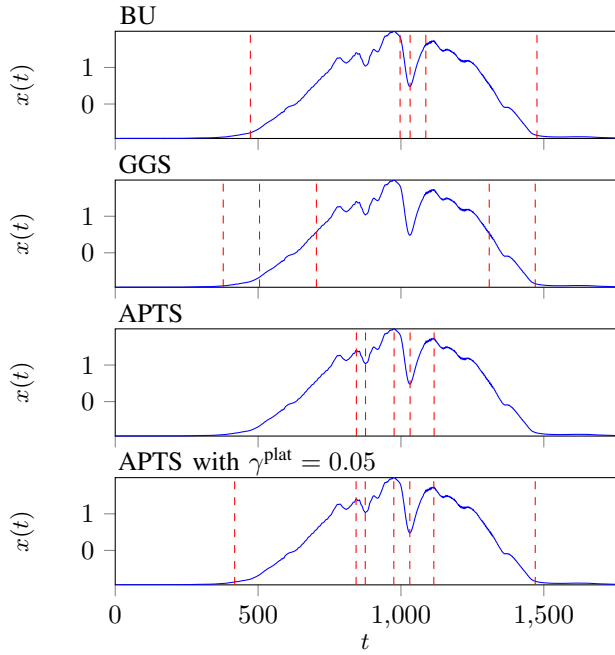


Fig. 5. Example 4. One-dimensional sample from dataset 'EthanoLevel' [24]. Default APTS comes with  $\gamma^{\text{plat}} = 0$ . The effect of  $\gamma^{\text{plat}} = 0.05$  is shown in the bottom subplot.

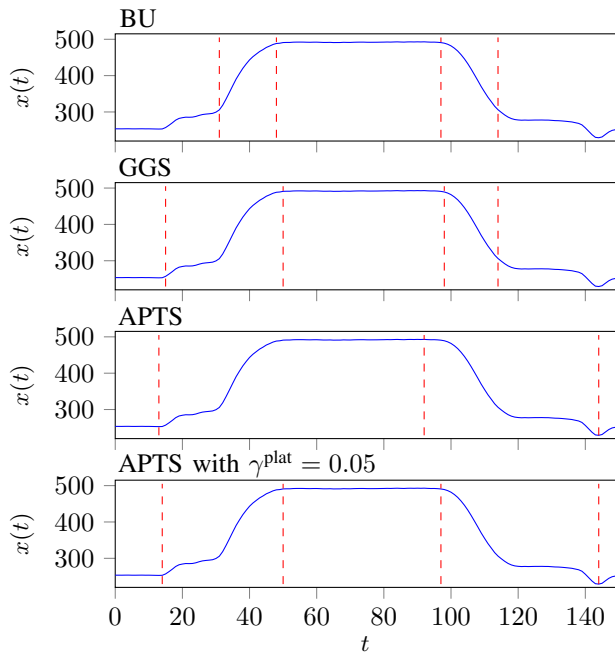


Fig. 6. Example 5. One-dimensional sample from dataset 'Gun-PointAgeSpan' [24]. Default APTS comes with  $\gamma^{\text{plat}} = 0$ . The effect of  $\gamma^{\text{plat}} = 0.05$  is shown in the bottom subplot.

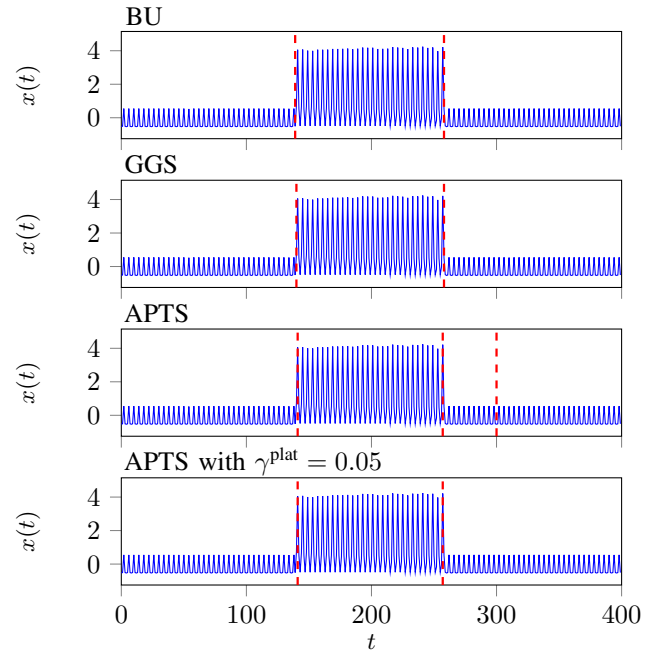


Fig. 7. Example 6. One-dimensional sample from dataset 'ACSF1' [24]. The effect of  $\gamma^{\text{plat}} = 0.05$  is further elaborated in Fig. 8.

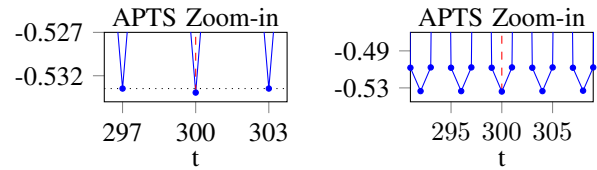


Fig. 8. Example 6. (Left) The zoom-in on the APTS-solution of Fig. 7 illustrates that the breakpoint at  $t = 300$  was identified for representing an outlier that is slightly smaller than all other neighboring local minima. The level of neighboring local minima is emphasized by the dotted horizontal line. (Right) The zoom-in shows that there are three data points around each local minimum. By setting  $\gamma^{\text{plat}} = 0.05$  the outlier is filtered out and the solution indicated in the bottom subplot of Fig. 7 is obtained.

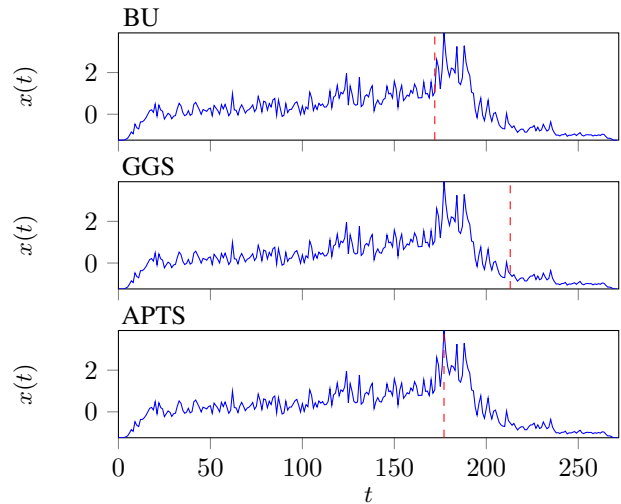


Fig. 9. Example 7. One-dimensional sample from dataset 'Lightning7' [24]. The breakpoint returned by APTS is exactly at the peak. BU does not set its breakpoint exactly at the peak. GGS segments two regions of different average amplitude levels.

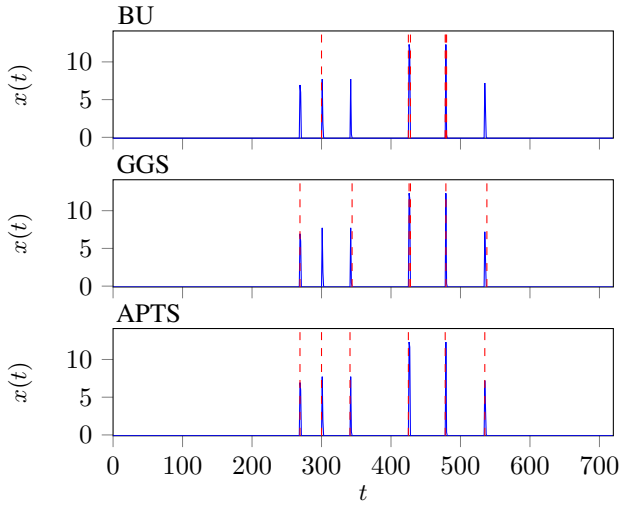


Fig. 10. Example 8. One-dimensional sample from dataset 'SmallKitchenAppliances' [24]. Only APTS identifies all six impulses correctly. In contrast, for both BU and GGS in at least one case two breakpoints are mapped closely to the same impulse.

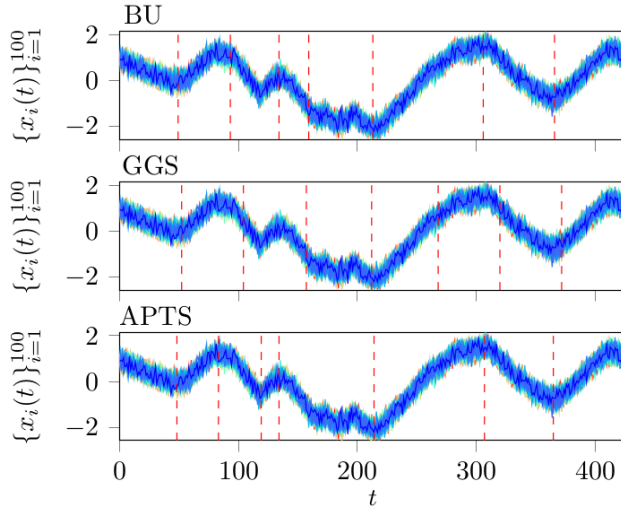


Fig. 11. Example 9. A one-dimensional sample from dataset 'Yoga' [24] is perturbed by zero-mean Gaussian noise with standard deviation of 0.2 to produce  $n_x = 100$  different time series.

It is found that *model-based* approaches such as BU [1] and GGS [2] are limiting, and not well generalizable to different shapes of data. For instance, the segmentation produced by GGS for the example in Fig. 2 is not intuitive. Likewise, BU produces unsuitable results in Fig. 3. It therefore appears that a *model-free* approach, such as APTS, is the most suitable choice to cover a large variety of different shapes of data. In a future extending hierarchical framework, on-top of a segmentation returned by APTS different models may be fitted to different segments.

For multivariate time series data the final segmentation returned by APTS is equally valid over all channels. However, before reaching consensus separate segmentations are obtained separately for each channel as part of the solution methodology. This property may be useful for extending upstream tasks such as time series clustering. This is pointed

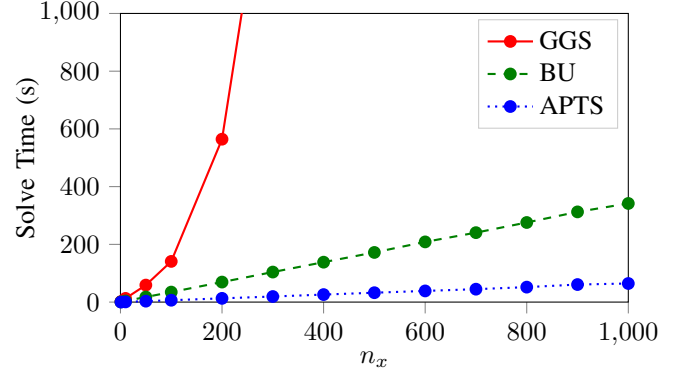


Fig. 12. Large-scale Example 10. The full dataset 'HandOutlines' [24] has 1000 channels and 2709 data points per channel. While keeping  $T = 2709$  constant, BU, GGS and APTS were applied to subsets of the data with  $n_x \in \{1, 10, 50, 100, 200, \dots, 1000\}$ , while recording the solve times. The y-axis is cut-off at 1000s solve time for clarity. See also Table II for more detailed numerical results.

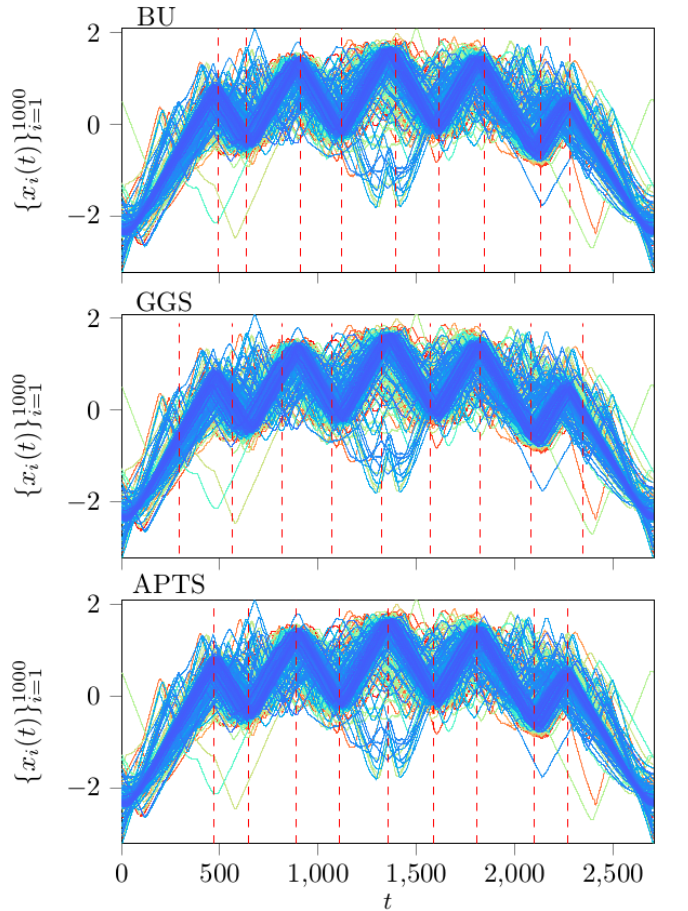


Fig. 13. Large-scale Example 10. Results for the full dataset 'HandOutlines' [24] are displayed. There are  $n_x = 1000$  channels with  $T = 2709$  data points for each channel.



Ex.	$n_x$	$T$	Solve Times (s)		
			BU [1]	GGs [2]	APTS
1	1	100	0.016	0.089	<b>0.002</b>
2	1	100	0.017	0.116	<b>0.002</b>
3	1	426	0.077	0.903	<b>0.010</b>
4	1	1751	0.369	2.293	<b>0.040</b>
5	1	150	0.026	0.161	<b>0.003</b>
6	1	400	0.073	0.081	<b>0.025</b>
7	1	272	0.048	0.017	<b>0.012</b>
8	1	720	0.135	0.405	<b>0.039</b>
9	100	426	5.267	24.75	<b>1.267</b>
10	50	2709	17.58	58.90	<b>3.19</b>
10	500	2709	172.0	7452.8	<b>32.47</b>
10	1000	2709	341.7	65847.5	<b>64.4</b>

TABLE II. Comparison of solve times in seconds. The last three rows show results for the same Example 10, but for a different number of channels  $n_x$ . For GGS with  $n_x = 500$  and  $n_x = 1000$  solve times are equivalent to more than 2h and 18h, respectively. APTS can solve the full dimensional Example 10 with  $n_x = 1000$  in approximately the same time, 64.4s, as GGS requires for its solution with  $n_x = 50$ . See also Fig. 13. Default APTS comes with  $\gamma^{\text{plat}} = 0$ . The solve times for Examples 4-6 with  $\gamma^{\text{plat}} = 0.05$  were 0.249s, 0.003s, 0.059s, respectively.

out since this is in contrast to GGS, where this property is absent and where only a combined segmentation over all channels is returned.

## V. CONCLUSION

A simple and scalable model-free algorithm for multivariate time series segmentation was presented. After a normalization step time series are treated channel-wise as surrogate stock prices that can be traded optimally a posteriori in a virtual portfolio holding either stock or cash. Linear transaction costs are therefore interpreted as hyperparameters for noise filtering. The resulting trading signals as well as the resulting trading signals obtained on the reversed time series are used for unsupervised labeling, before a consensus over channels is reached that finally determines segmentation time instants. Proposed algorithm is called *A posteriori Trading-inspired Segmentation* (APTS) and was compared to a popular bottom-up approach [1] fitting piecewise affine models and to a recent top-down approach fitting Gaussian models [2] on a variety of different synthetic data as well as real-world datasets from the UCR time series archive [24]. Overall, APTS was found to be consistently faster while producing more intuitive segmentation results.

There are two main avenues for future work. First, the method may be extended for recursive online time series segmentation, for example, within a moving horizon framework and with special focus on the most recent segment. Second, the method may serve as foundation for further upstream time series analysis tasks such as clustering, compression and forecasting.

## REFERENCES

[1] E. Keogh, S. Chu, D. Hart, and M. Pazzani, "An online algorithm for segmenting time series," in *IEEE International Conference on Data Mining*, pp. 289–296, 2001.

[2] D. Hallac, P. Nystrup, and S. Boyd, "Greedy gaussian segmentation of multivariate time series," *Advances in Data Analysis and Classification*, vol. 13, no. 3, pp. 727–751, 2019.

[3] E. Keogh, S. Chu, D. Hart, and M. Pazzani, "Segmenting time series: A survey and novel approach," in *Data Mining in Time Series Databases*, pp. 1–21, World Scientific, 2004.

[4] S. Aminikhanghahi and D. J. Cook, "A survey of methods for time series change point detection," *Knowledge and Information Systems*, vol. 51, no. 2, pp. 339–367, 2017.

[5] C. Truong, L. Oudre, and N. Vayatis, "Selective review of offline change point detection methods," *Signal Processing*, p. 107299, 2019.

[6] F. Desobry, M. Davy, and C. Doncarli, "An online kernel change detection algorithm," *IEEE Transactions on Signal Processing*, vol. 53, no. 8-2, pp. 2961–2974, 2005.

[7] K. D. Feuz, D. J. Cook, C. Rosasco, K. Robertson, and M. Schmitter-Edgecombe, "Automated detection of activity transitions for prompting," *IEEE Transactions on Human-Machine Systems*, vol. 45, no. 5, pp. 575–585, 2014.

[8] Y. Zheng, L. Liu, L. Wang, and X. Xie, "Learning transportation mode from raw gps data for geographic applications on the web," in *International Conference on World Wide Web*, pp. 247–256, ACM, 2008.

[9] F.-L. Chung, T.-C. Fu, V. Ng, and R. W. Luk, "An evolutionary approach to pattern-based time series segmentation," *IEEE Transactions on Evolutionary Computation*, vol. 8, no. 5, pp. 471–489, 2004.

[10] Y. Kawahara, T. Yairi, and K. Machida, "Change-point detection in time-series data based on subspace identification," in *IEEE International Conference on Data Mining*, pp. 559–564, 2007.

[11] R. P. Adams and D. J. MacKay, "Bayesian online changepoint detection," *arXiv preprint arXiv:0710.3742*, 2007.

[12] E. Fuchs, T. Gruber, J. Nitschke, and B. Sick, "Online segmentation of time series based on polynomial least-squares approximations," *IEEE Transactions on Pattern Analysis and Machine Intelligence*, vol. 32, no. 12, pp. 2232–2245, 2010.

[13] Z. Harchaoui, F. Vallet, A. Lung-Yut-Fong, and O. Cappé, "A regularized kernel-based approach to unsupervised audio segmentation," in *IEEE International Conference on Acoustics, Speech and Signal Processing*, pp. 1665–1668, 2009.

[14] W.-H. Lee, J. Ortiz, B. Ko, and R. Lee, "Time series segmentation through automatic feature learning," *arXiv preprint arXiv:1801.05394*, 2018.

[15] H. Chen, N. Zhang, *et al.*, "Graph-based change-point detection," *The Annals of Statistics*, vol. 43, no. 1, pp. 139–176, 2015.

[16] S. Liu, M. Yamada, N. Collier, and M. Sugiyama, "Change-point detection in time-series data by relative density-ratio estimation," *Neural Networks*, vol. 43, pp. 72–83, 2013.

[17] Y. Kawahara and M. Sugiyama, "Sequential change-point detection based on direct density-ratio estimation," *Statistical Analysis and Data Mining: The ASA Data Science Journal*, vol. 5, no. 2, pp. 114–127, 2012.

[18] J. Himberg, K. Korpiaho, H. Mannila, J. Tikanmaki, and H. T. Toivonen, "Time series segmentation for context recognition in mobile devices," in *IEEE International Conference on Data Mining*, pp. 203–210, 2001.

[19] A. Garg, L. Manikonda, S. Kumar, V. Krishna, S. Boriah, M. Steinbach, V. Kumar, D. Toshniwal, C. Potter, and S. Klooster, "A model-free time series segmentation approach for land cover change detection," in *NASA Conference on Intelligent Data Understanding*, 2011.

[20] R. Agrawal, C. Faloutsos, and A. Swami, "Efficient similarity search in sequence databases," in *International Conference on Foundations of Data Organization and Algorithms*, pp. 69–84, Springer, 1993.

[21] M. Sharifzadeh, F. Azmoodeh, and C. Shahabi, "Change detection in time series data using wavelet footprints," in *International Symposium on Spatial and Temporal Databases*, pp. 127–144, Springer, 2005.

[22] X. Liu, Z. Lin, and H. Wang, "Novel online methods for time series segmentation," *IEEE Transactions on Knowledge and Data Engineering*, vol. 20, no. 12, pp. 1616–1626, 2008.

[23] M. G. Plessen and A. Bemporad, "A posteriori multistage optimal trading under transaction costs and a diversification constraint," *The Journal of Trading*, vol. 13, no. 3, pp. 67–83, 2018.

[24] H. A. Dau, A. Bagnall, K. Kamgar, C.-C. M. Yeh, Y. Zhu, S. Gharghabi, C. A. Ratanamahatana, and E. Keogh, "The UCR time series archive," *arXiv preprint arXiv:1810.07758*, 2018.

[25] R. Bellman *et al.*, "The theory of dynamic programming," *Bulletin of the American Mathematical Society*, vol. 60, no. 6, pp. 503–515, 1954.

[26] D. Q. Goldin and P. C. Kanellakis, "On similarity queries for time-series data: constraint specification and implementation," in *International Conference on Principles and Practice of Constraint Programming*, pp. 137–153, Springer, 1995.